The timing of the penultimate glaciation in the northern Alpine Foreland: new insights from luminescence dating

Lukas Bickel [a,*], Christopher Lüthgens [a], Johanna Lomax [b], Markus Fiebig [a]

[a] *Institute of Applied Geology, Department of Civil Engineering and Natural Hazards, University of Natural Resources and Life Sciences, Peter Jordan-Straße 70, 1190 Vienna, Austria*
[b] *Department of Geography, Justus-Liebig-University Giessen, Senckenbergstraße 1, 35390 Giessen, Germany*

A B S T R A C T

Only minimal age constraints are as yet available concerning the timing of the penultimate glaciation in the European Alps. Therefore, this study presents the results of different luminescence dating approaches, revealing the depositional ages of glaciofluvial sediments deposited in the Austrian Northern Alpine Foreland during the penultimate glaciation. To establish a robust numerical chronology we investigated 18 samples of mostly glaciofluvial origin using the optically stimulated luminescence (OSL) signal of quartz and the post-infrared infrared (pIRIR) stimulated luminescence signal at 225 °C of potassium rich feldspar for the grain size of 100–200 μm. By comparing the results gained from both analytical approaches, it was possible to discern between samples that were well bleached prior to deposition and samples for which the luminescence signals were not properly reset. The ages presented in this study suggest that the deposition of proglacial outwash deposits in the northern Alpine foreland associated with the penultimate glaciation is time equivalent with marine isotope stage (MIS) 6. Furthermore, our results imply relatively rapid ice decay in late MIS 6 towards termination 2, which is consistent with previous studies dealing with the penultimate glaciation in the circum-alpine region. Although the dating results allow to chronologically discern between glacial and interglacial periods, a finer resolution on a stadial/interstadial level cannot unfortunately be obtained by the current state-of-the-art methods of luminescence dating as applied in this study.

1. Introduction

The Quaternary sedimentary legacy of the Northern Alpine Foreland (NAF) plays a key role when it comes to deciphering the Middle and Late Pleistocene history of the Alps. First theories about an extensive glaciation in the alpine region were already developed in the 18th and 19th century by several natural scientists (e.g. Agassiz, 1841). Penck and Brückner (1909) established a quadriglacial theory for the Alps based on a vertical fluvial terrace succession deposited in connection to a glacial system in the hinterland (from old to young: Günz, Mindel, Riss, Würm). Since then, this morphostratigraphic model was regionally amended and enhanced. In Austria, the quadriglacial system is still the foundation for the Quaternary stratigraphy as no clear chronostratigraphic succession can be concluded for presumably older Quaternary deposits (e.g. Eichwald gravel; Weinberger, 1955;

Van Husen and Reitner, 2011). During each of the four glaciations inferred from field evidence in the Austrian Eastern Alps and its foreland, the spatial glacier extent and lateral glacier advance gradually decreased from west to east. While the Salzach Glacier in the West of the Austrian NAF was a piedmont glacier *sensu stricto* during the last glaciation, the eastern glaciers roughly reached the morphological alpine border or were even confined to localized alpine amphitheatres (palaeogeographic reconstruction in Van Husen (2011a, 2011b)). The sediments deposited by meltwater streams characterize the glaciofluvial geomorphological elements of the North-eastern Alpine Foreland. Nowadays, the deposits of the two oldest glaciations form elevated gravel plateaus due to general tectonic uplift of the area. The glaciofluvial remnants of the youngest two glaciations are imbedded into erosional channels forming river valley terraces. The timing of the four glaciations was tentatively correlated with equivalent marine isotope stages (MIS), using various stratigraphic approaches (i.e. morphostratigraphy, biostratigraphy, etc.), as outlined by Van Husen and Reitner (2011) – although it should be stressed that evidence from numerical dating is scarce. As glacial landscapes are often subject to thorough

reworking and erosion, direct correlation of the continuous marine isotope stage (MIS) records with discontinuous glacial and glaciofluvial terrestrial records is obviously not trivial. Additionally, when the formation of fluvial gravel plains and terraces may be influenced by tectonic processes, their climatic significance is not clear in some cases. The only way to solve this problem is to establish an independent numerical chronology. The evolution of luminescence dating techniques during the last few years has allowed for depositional ages of sedimentary deposits of up to 300–400 ka and up to 1 Ma in some cases – depending on environmental conditions and applied techniques (e.g. Preusser et al., 2008; Rhodes, 2011). This theoretically allows the dating of Middle Pleistocene glaciofluvial sediments of the NAF. In this region, the stratigraphic approaches for the penultimate glaciation vary: while recent approaches in the western part of the NAF divide the penultimate glaciation (termed "Riss") glaciation into two discrete glacials divided by an interglacial (Miara, 1996; Ellwanger et al., 2011), the Austrian stratigraphic chart only attributes one glacial stage to the Riss. It is not clear if this is an artefact of fragmentary sedimentary records and numerical chronologies or of climatic gradients from the central to the eastern part of the NAF. To answer these questions, establishing new accurate numerical ages of the sedimentary legacy of the glaciations is required. In the central region of the Austrian NAF (Traun-Enns plateau), the connection of glaciofluvial terraces with terminal moraines is very well recognized (Penck and Brückner, 1909; Kohl, 2000). This area is therefore ideal to reconstruct the timing and extent of Quaternary Alpine glaciations through age determinations of the terraces using luminescence dating. We chose to mainly focus our dating efforts on the glaciofluvial continuation of the penultimate glacial deposits in the Austrian NAF. The so-called "Hochterrasse" (Eng.: High Terrace) is interpreted as representing the coarse, gravelly meltwater accumulations deposited by braided rivers during the penultimate glacial cycle (Penck and Brückner, 1909; Van Husen and Reitner, 2011). The minimum age for this is at least 130 ka (Van Husen and Reitner, 2011), which poses a challenge for age control using independent methods. On the one hand, radiocarbon with an upper dating limit of c. 45 ka is not suited for such old deposits. On the other hand, U/Th, which can be used to date calcitic cements and crusts of the gravel deposits, only yield ages which are representative for the time of calcite formation but not the depositional age of the sedimentary body itself. Therefore we applied a twofold dating approach, using the OSL signal of quartz and the post infrared infrared stimulated (pIRIR) signal of K-feldspars to perform internal cross-checks nonetheless. This approach has already been successfully applied in a study by Bickel et al. (2015). A first attempt to date the High Terrace deposits of the German NAF by luminescence methods was undertaken by Klasen (2008), but anomalous fading of feldspar and unfavourable signal composition of quartz prevented a well-defined chronostratigraphic classification. Recently, Roskosch et al. (2015) have successfully applied IRSL methods for ice marginal samples from Northern Germany ranging from MIS 6 to MIS 12. In this paper we (1) apply luminescence methods to date proximal glaciofluvial sediments, (2) assess the presence of partial bleaching and reliability of quartz OSL and feldspar pIRIR in order to (3) discuss the stratigraphic implications of the new ages in context with earlier regional and supra-regional studies.

2. Sampling sites

Eight locations were studied, and a total of 18 samples collected for luminescence dating from ice marginal deposits, piedmont terraces and covering loess-palaeosol sequences (Fig. 1). With the exception of one deltaic deposit and the eolian covering layers,

the fluvial sediments were deposited by a braided river system. The exposures were investigated on site regarding sedimentary structures, petrographic composition and lithostratigraphy. Vertical lithostratigraphic profiles of the sites are shown in Fig. 2. The abbreviations the subheadings refer to locations marked in Fig. 1. Coordinates and elevation data are given in Table 1. In the following, the investigated sites are grouped according to their respective glacial catchment area and internally listed from ice proximal to distal locations.

2.1. Oberrohr (Krems Glacier: Kr1, Fig. 2a)

Glaciofluvial terrace sediments of the Krems valley attributed to the penultimate glaciation are exposed at Oberrohr. A c. 9 m thick succession of poorly sorted, horizontally bedded, medium braided river gravels can be roughly subdivided into an upper thoroughly cemented conglomerate (0–3 m) and a lower (3–12 m) granular gravel. The lithology is dominated by carbonatic components, but with a fairly high amount of sandstone (c. 10–20%, field estimate). Two samples for luminescence dating were taken from elongated sand lenses (ORO1, ORO2).

2.2. Sierninghofen (Steyr Glacier: St1, Fig. 2b)

An extensive gravel pit at Sierninghofen exposes up to 45 m of horizontally stratified, glaciofluvial braided river deposits of the lower Steyr valley. The well rounded, clast supported, sandy coarse gravels rarely show planar cross stratification. The petrographic composition consists mostly of material derived from the Northern Calcareous Alps and the Flysch zone (an overview of the Austrian tectonic units can be found in Schuster et al., 2014). Occurrence of crystalline rocks of the Central Eastern Alps (Lower Tauern) is rare. During mining, big, subangular blocks were excavated. Most likely, they should be interpreted as ice rafted debris, implying proximity to a glacier front. Based on conglomeration, the pit wall can be subdivided into three regions. Cementation of clasts in the highest 15 m and the lowest 22 m is very limited. The middle part in between however is strongly cemented. Sand lenses suitable for luminescence dating were rare, apart from two lenses in the upper part of the gravel succession where two samples were collected from the same stratigraphic depth (SRN1, SRN2). An auburn clayey palaeosol lies unconformably above the gravel deposits, retracing the underlying palaeo-relief. The top of the vertical profile consists of carbonate-free silty to fine sandy loess loam. The original top of the sedimentary succession was stripped in the course of the mining process. Therefore the original thickness of the loess succession is unknown.

2.3. Dörfling (Enns Glacier/Steyr Glacier: En1, Fig. 2c)

High Terrace gravels of the lower Enns valley are exposed in a c. 10 m vertical pit face at Dörfling. Compared to the petrographic composition of the gravel deposits of Sierninghofen (13 km southwest) the clast supported gravels of Dörfling show an increase of macroscopic crystalline clasts. Rare sand lenses and layers with a considerable amount of fine to medium gravel can be observed. Three of these sand deposits were sampled for luminescence dating (DRF1, DRF3, DRF4). Towards the top, the gravel succession shows gradually intensifying weathering colours which culminate in a thin, discordantly overlying palaeosol. Above this, lies a carbonate free loess loam sequence which shows reworking and a hydromorphic overprint (Fe- and Mg-hydroxide precipitates) in the basal 20–30 cm. The loess sequence gradually merges into a modern day calcareous cambisol. A loess sample (DRF2) was collected for luminescence dating.
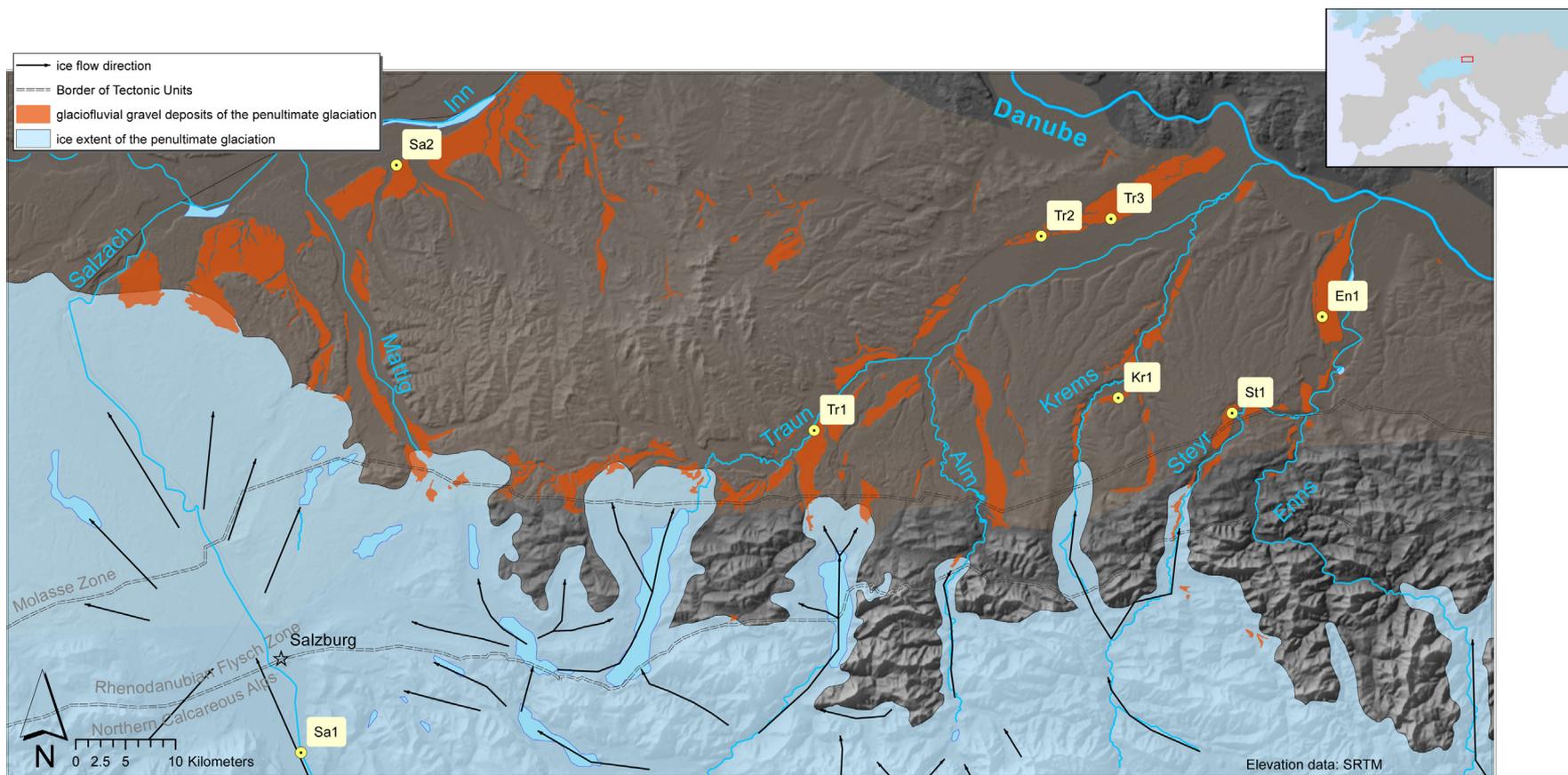
Fig. 1. Overview map of the investigated area. The red areas depict the extent of the glaciofluvial gravel accumulations of the penultimate glaciation (Krenmayr et al., 2006), their maximum extent is shown in light blue, including ice flow directions indicated by arrows. The small inlet shows the ice extent of the Alps and Northern Europe during the penultimate glaciation (Ehlers and Gibbard, 2004). The investigated sites are displayed with their abbreviation: Sa1 = Urstein, Sa2 = Appersting, Tr1 = Desselbrunn, Tr2 = Unterhart, Tr3 = Hörsching, Kr1 = Oberrohr, St1 = Sierninghofen, En1 = Dörfling.

Fig. 2. Lithostratigraphic sections of the investigated sites. Facies codes c.f. Miall (2006). Gh = clast supported, crudely, planar bedded gravel; Gt = gravel, trough cross-beds; Gp = gravel, planar cross-beds; Sh = sand, horizontally laminated; Sp = sand, planar cross-beds; L = loess; S = soil (recent); P = palaeosol.
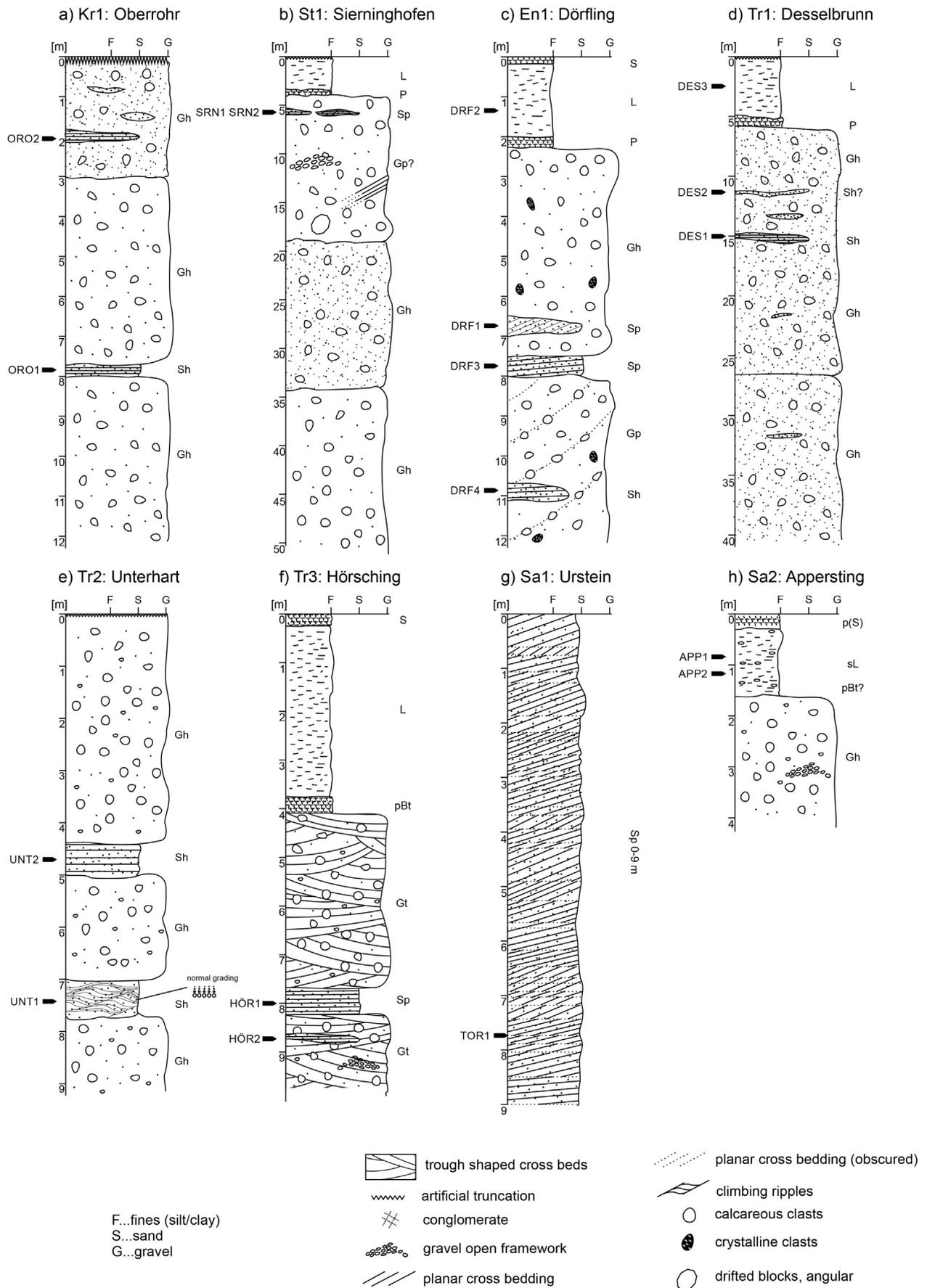
Table 1
Radionuclide data of the investigated samples as well as their location (UTM 33N) and elevation a.s.l. including burial depth. The effective dose rate (Dr_{eff}) comprises the environmental and cosmic dose rate.

Site	Sample	UTM 33N northing	UTM 33N easting	m a.s.l.	m b.g.l.	K40 [%]	±	Th232 [ppm]	±	U238 [ppm]	±	Dr_{eff} [Gy ka^{-1}]
En1	DRF1	5331058	458570	537.0	7.0	0.16	0.00	0.70	0.03	3.06	0.06	0.89
En1	DRF2	5331058	458570	364.5	1.5	1.64	0.04	13.58	0.35	4.10	0.08	3.22
En1	DRF3	5331055	458567	364.8	1.2	0.34	0.01	1.26	0.05	2.36	0.05	0.92
En1	DRF4	5331055	458567	407.0	15.0	0.91	0.02	1.69	0.04	4.09	0.12	1.42
St1	SRN1	5321397	449467	410.0	12.0	0.12	0.00	0.45	0.02	1.93	0.04	0.76
St1	SRN2	5321397	449467	419.5	2.5	0.11	0.00	0.44	0.02	1.93	0.04	0.62
Kr1	ORO1	5322931	438129	303.5	7.5	0.69	0.02	3.30	0.11	1.54	0.04	1.17
Kr1	ORO2	5322931	438129	306.4	4.6	0.77	0.02	4.52	0.14	1.90	0.04	1.41
Tr1	DES1	5319669	407632	290.0	8.0	0.37	0.01	2.00	0.07	1.12	0.03	0.69
Tr1	DES2	5319669	407632	289.2	8.8	0.27	0.01	1.38	0.05	1.33	0.03	0.63
Tr1	DES3	5319669	407632	344.1	7.9	1.45	0.03	12.78	0.34	3.53	0.08	3.04
Tr2	UNT1	5339058	430380	350.0	2.0	0.70	0.00	2.50	0.04	1.09	0.02	0.85
Tr2	UNT2	5339065	430454	346.2	5.8	0.74	0.02	2.42	0.08	1.27	0.03	1.07
Tr3	HOR1	5340835	437347	346.2	5.8	0.31	0.01	1.46	0.06	1.40	0.03	0.71
Tr3	HOR2	5340947	437338	290.3	6.7	0.42	0.01	1.73	0.06	1.23	0.03	0.78
Sa1	TOR1	5287410	356299	295.6	1.4	0.85	0.02	4.43	0.13	1.25	0.03	1.31
Sa2	APP1	5353201	410701	289.3	7.7	1.04	0.02	9.58	0.26	2.97	0.06	2.86
Sa2	APP2	5353201	410701	286.1	10.9	1.11	0.02	10.54	0.28	3.28	0.07	3.15

2.4. Desselbrunn (Traun Glacier: Tr1, Fig. 2d)

A gravel pit c. 6.5 km north of the terminal moraine ridges of the penultimate glaciation in the Traun valley exposes 35 m of glaciofluvial, sandy, coarse conglomerates of the High Terrace. Scattered, thin sand lenses (concentrated in the upper half of the succession), as well as the gravels themselves, are horizontally bedded. Two samples were taken from two sand lenses located in the upper 12 m of the succession (DES1, DES2). A palaeosol-loess sequence is situated discordantly above the gravels filling morphological depressions. An additional sample was taken from the overlying loess deposit (DES3).

2.5. Unterhart (Traun Glacier: Tr2, Fig. 2e)

30 km downstream of Tr1, the sediments of the glaciofluvial High Terrace of the Traun valley are exposed in Unterhart in a c. 9 m thick succession. Poorly sorted, horizontally bedded, sandy gravels are often interrupted by thin sand lenses. At the vertical section, two sand lenses were deemed thick enough for OSL sampling (UNT1, UNT2). The lower sand lens consists of light grey, cross-stratified, fining upward medium to fine sand interbeds (Fig. 3B), whereas the fabric of the upper lens is more or less tight-bedded with mm-scale horizontal laminations in the lower part with occasional scattered fine to medium gravels.

2.6. Hörsching (Traun Glacier: Tr3, Fig. 2f)

The gravel pit of Hörsching, 7 km downstream of the Unterhart site, exposes c. 6 m of medium to coarse gravels of the same terrace body. Trough cross stratification is clearly identifiable in two perpendicular pit faces (Fig. 3C), indicating flow direction towards NE. Grain size variability is evident, ranging from grain supported sandy gravels to open-framework gravels. Thin, horizontally laminated, fine to medium sand layers and lenses were recorded interbedded within the gravels. The bottom of the sand lenses is rich in fine gravel components which gradually diminish to a few scattered gravels within the bottom 5 cm. Two samples for luminescence dating were taken from two individual sand lenses (HOR1, HOR2). Reddish iron oxide weathering colours intensify in the top where 30–50 cm of auburn, clayey palaeosol are exposed. Above lie roughly 3 m of carbonate free loess loam, topped by a thin band of modern day in situ soil.

2.7. Urstein (Salzach Glacier: Sa1, Fig. 2g)

Sample TOR1 was taken from an outcrop situated at the Salzach River. The outcrop exposes 9 m of sandy, medium- to well-rounded gravel (mostly calcareous) in various states of cementation (Fig. 3A). Occasionally pure medium to coarse sand beds can be observed. The cm to dm thick, normal graded beds are dominated by planar cross beds with northward dipping foresets. This site is attributed to the local stratigraphic unit of the "Torrener Nagelfluh" (Torren conglomerate, Van Husen and Reitner, 2011), interpreted as sediment deposited into an ice marginal lake forming a delta complex. At its locus typicus, deltaic clinoform foresets in the lower part and horizontal, cross stratified top sets in the top part (which is exposed at Urstein) formed in a lake between stagnant ice and the slope during the deglaciation of the penultimate glaciation (Termination II; Van Husen, 2000; Van Husen and Reitner, 2011). A sample block of 50 × 30 × 30 cm was cleared out of the outcrop wall to be processed for luminescence dating (TOR1).

2.8. Appersting (Salzach Glacier: Sa2, Fig. 2h)

The site is located in an abandoned gravel pit in the High Terrace south of the river Inn (synonymous with the site "Gunderding" by Terhorst et al., 2002). The collapsed pit walls gave no opportunity to collect a useful OSL sample from within the terrace gravels, instead two samples were collected from the covering loess loam layer (APP1, APP2). This overlying soil formation was previously attribute to the Eemian interglacial based on U/Th dating of secondary calcite cements found in the underlying terrace body (Gunderding site, MIS 5e, Terhorst et al., 2002). On spots, where the original sedimentary succession of the lower part was exposed, uncemented, clast supported gravel with a coarse-sandy matrix was recorded. Open-framework gravels were recorded as well – typical indicators for a braided river system (Bridge and Lunt, 2006). Imbricated clasts indicate a palaeo-flow-direction towards the east, and similar to the present day Inn River course. Scattered gravel clasts within the discordantly overlying loess imply aqueous reworking of the silty sediment. The sedimentary succession is concluded by a recent pseudogley.

Fig. 3. Photographs of selected representative sites. White arrows indicate sampling spots. (A) Sa1 deltaic sequence. The sediments are dominated by cemented, medium to coarse sands with occasional intercalations of fine-medium gravel laminae. The stratification is characterized by planar cross beds with truncated tops. A sample block was carved out of the lowermost exposed area. (B) Characteristic glaciofluvial deposit of the Austrian NAF at site Tr2. Sand lenses and beds with limited horizontal extent (dotted lines) were sampled for luminescence dating. Massive deposits of coarse, crudely planar bedded gravels cut discordantly in the small sand accumulations. (C) Gravel deposit (Tr3) showing trough cross bedding with intercalated sand lenses. An intercalated sand lens (arrow) was sampled for luminescence analysis.

3. Methods

3.1. Sample preparation

Samples for luminescence dating were obtained by driving steel cylinders into unconsolidated sand and silt layers. The laboratory preparations for dating were performed under darkroom conditions using only subdued red light. After dry sieving (100–200 μm), the samples were treated with 10% HCl and 15% H_2O_2 to remove carbonates and organic matter. The in situ taken block of site Sa1 (TOR1) was treated differently: to remove sunlight exposed parts of the block, black spray paint was used to completely cover the original surface. Subsequently the outer 1–2 cm of the block were removed in the lab using hammer and chisel, until the painted parts were fully removed. For this sample, sieving was done after treatment with HCl and H_2O_2. Sodium oxalate was added to deflocculate mineral aggregates. To isolate Quartz (Q) and K-Feldspar (KFs) fractions, the samples were gravity separated using lithium tungstate heavy liquid (2.58 g/cm^3 and 2.68 g/cm^3). The quartz separates were subsequently etched with 40% HF, rinsed in 15% HCl and sieved at 100 μm. For measurements, KFs and Q grains were mounted on stainless steel discs (∅ 9.7 mm), where the aliquots covered the central 1 mm for KFs and 2 mm for Q. Samples for gamma spectrometry were disintegrated with mortar and pestle where necessary, and sealed in air-tight 250 ml Marinelli beakers for at least 2 weeks to ensure secular Radon equilibrium before measurement.

3.2. Dose rate measurements

A Germanium detector gamma spectrometer (40% n-type) was used to measure the dose relevant environmental radionuclides (40K, 232Th, 238U). Cosmic radiation contribution was estimated using calculations of Prescott and Hutton (1994). For coarse grain KFs an alpha efficiency of 0.07 ± 0.02 was used (Klasen, 2008) and an internal potassium content of $12.5 \pm 0.5\%$ was assumed (c.f. Huntley and Baril, 1997). To account for radiation attenuation by pore water, the samples were dried at 80 °C to assess the present day water content. As expected due to mining activities at all sites, the current water content in the samples is relatively low. The lack of knowledge about the timing of changes in the hydrologic systems at the sites, river incision and lowering of the groundwater table, make it impossible to reliably determine a water content which is representative for the whole time span of burial. For this reason a water content of $15 \pm 10\%$ was used to cover the possible conditions (reaching from almost dry to almost saturated). Radionuclide contents of the investigated samples are shown in Table 1.

3.3. Luminescence measurements

For information on the fundamental principles of luminescence dating, we refer to the comprehensive works by Aitken (1998) and Bøtter-Jensen et al. (2003). Luminescence signals were stimulated and recorded by two automated Risø TL/OSL-DA-20 luminescence readers, each equipped with a 90Sr/90Y beta source delivering a dose rate of 0.10 and 0.13 Gy/s. An array of blue LEDs (470 nm, $\sim$41 mW cm^{-2} @ 100% power) was used to stimulate luminescence in quartz (40 s @ 125 °C), which was detected and recorded by a photomultiplier tube (PMT) through an ultraviolet transmitting Hoya U340 filter (7.5 mm). KFs separates were stimulated by IR diodes (870 nm, 300 s @ 50 °C and 225 °C respectively) and the signal was detected by PMT after passing a 410/30 interference filter (2 mm).

Standard single aliquot regenerative dose (SAR) protocols (Wintle and Murray, 2006) were used to determine equivalent doses (D_e) from Q, including IR stimulation after short artificial irradiation ($\sim$20 Gy) at the end of the measurement sequence to identify possible feldspar contaminations. A characteristic OSL decay and dose–response curve is given in Fig. 4. Q-aliquots that showed a significant signal response to IR stimulation were excluded from further analysis. A post-infrared-infrared approach at 225 °C stimulation temperature (Buylaert et al., 2009) was used for KFs D_e determination. The 50 °C signal of the aforementioned protocol was also investigated, but due to inherent problems of anomalous fading (signal loss with time; Wintle, 1977) and its

correction, the data are not deemed viable for reliable chronological interpretations (c.f. Bickel et al., 2015). The fading rates Auclair et al., 2003) were determined for at least one sample per site to estimate the impact of anomalous fading on the pIRIR signal. Dose altering effects of unbleachable residual doses were investigated by exposing samples to direct sunlight for a prolonged time (up to three day/night cycles) and measuring the residual signal with a standard SAR protocol afterwards. Combined dose recovery and preheat tests were performed for at least one sample per site to ensure reproducibility of artificial doses within a measurement protocol (180–280 °C for quartz and 190–290 °C for feldspar; 20 °C steps; 3 aliquots each). The tests revealed suitable preheating conditions for 60 s @ 250 °C for feldspar and for 10 s @ 260 °C with a 240 °C cut heat for quartz. These preheat conditions were applied in the routine D_e measurements. In addition to standard SAR quality criteria (10% recycling ratio, 10% test dose error, 5% recuperation, error >3 sigma above background), we applied additional "soft rejection criteria" for quartz, based on observations of the OSL decay curve geometry to mitigate the possible influence of thermally unstable signal components to a minimum (Bickel et al., 2015).

4. Results and discussion

4.1. Luminescence characteristics

The general luminescence properties are in good agreement with findings by Bickel et al. (2015). Fading experiments (c.f. Auclair et al., 2003) for seven samples (DRF1, DRF2, SRN1, SRN2, ORO1, HÖR1, HÖR2) revealed significant fading rates for the IR$_{50}$ signal of feldspars of the NAF (mean g-value of $3.3 \pm 0.8\%$) and negligible fading rates for the pIRIR$_{225}$ signal (g-values <1%), which are in consistency with fading rates of feldspar from glaciofluvial sediments of the Ybbs valley in the very East of the NAF (Bickel et al., 2015). A fading correction c.f. Huntley and Lamothe (2001) was not applied, because this kind of correction is only valid if the natural signals intersect the growth curve in its initial linear part, which was not the case for the bulk of the measured aliquots. Due to the relatively high-dosed nature of the samples (>150 Gy), we refrained from correcting the IR$_{50}$ ages for fading and based our chronological interpretations solely on the OSL and pIRIR$_{225}$ ages. For the sampled glaciofluvial sand, natural OSL and pIRIR are well below saturation levels. The natural OSL signal of the loess sample DRF2 shows signs of saturation for >50% of the measured aliquots and the rest are close to saturation levels. Therefore the OSL age of this sample must be regarded as minimum age, even though complete resetting can be assumed in this depositional environment. In view of high dose rates,
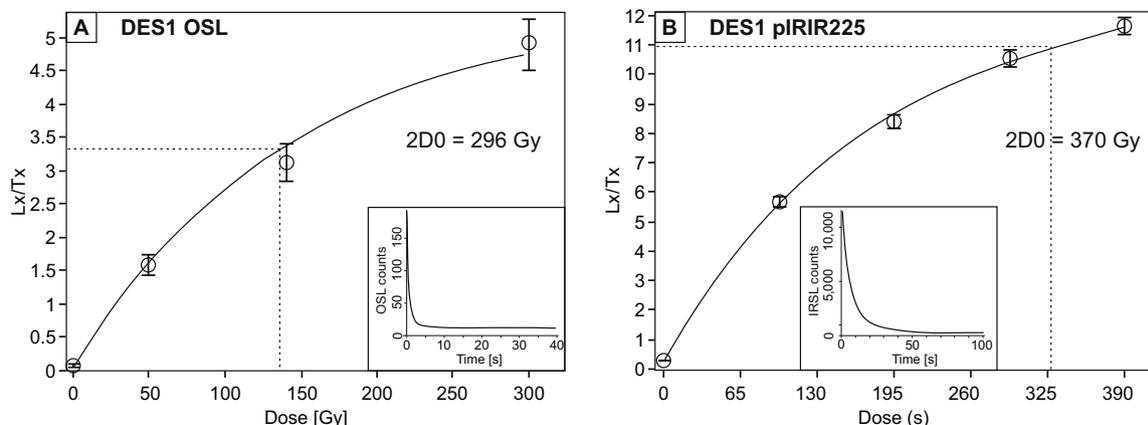

Fig. 4. Representative dose–response curve for an aliquot of sample DES1 using the OSL signal of quartz and the pIRIR signal of potassium feldspar. The inset shows the depletion of the natural signal during the first OSL read out. An exponential fit ($Y = a(1 - \exp[(x + c)/b])$) was used for the dose–response curve fit.
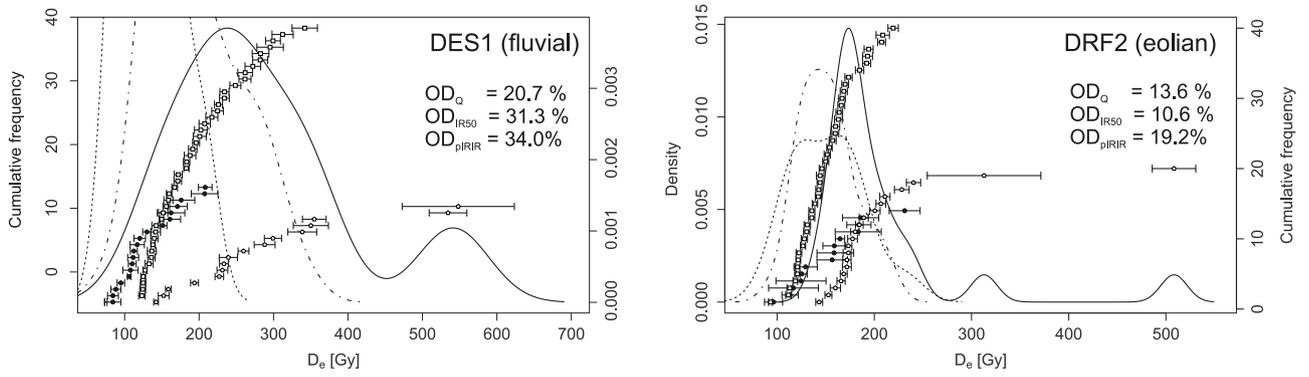
Fig. 5. Plots of the cumulative dose distribution and kernel density of a glaciofluvial (DES1) and an eolian (DRF2) sample for three signals (OSL (circles, dashed line) of quartz; IR50 (squares, dash-dotted line) and pIRIR225 (pentagons, solid line) for KFs). While the eolian sample shows a relatively narrow distribution of equivalent doses, the doses of the glaciofluvial sample are much wider spread. The OSL distribution for eolian DRF2 is rather scattered due to saturation effects.

high probability of complete resetting and low residual doses, KFs pIRIR$_{225}$ was therefore the preferred approach for the remaining loess samples.

4.2. Dose distributions, bleaching completeness and age calculation

We used the central age model (CAM) by Galbraith et al. (1999) for age calculations throughout this study, as dose distributions are largely symmetric and single peaked. The minimum age model for quartz (Galbraith et al., 1999) was not deemed applicable, as D_e distributions (e.g. Fig. 5) in this study are not significantly positively skewed and therefore it is appropriate to use the CAM (c.f. Bailey and Arnold, 2006).

Incomplete resetting of the luminescence signal can be a commonly observed feature in fluvial and especially glaciofluvial environments (Thrasher et al., 2009; Lüthgens et al., 2010, 2011; King et al., 2014). Empiric studies have proven, that the post-IR signal of K-feldspar bleaches at a slower rate than the low temperature IR50 signal (Starnberger et al., 2013; Kars et al., 2014;

Bickel et al., 2015). In contrast, the quartz OSL signal is known to bleach significantly faster than the aforementioned feldspar signals (Murray et al., 2012; Starnberger et al., 2013). Offsets in age between the three signals can therefore be seen as the result of incomplete signal resetting prior to deposition (Murray et al., 2012; Bickel et al., 2015) if dose altering effects (e.g. anomalous fading, residual doses) can be successfully mitigated. Residual doses of the post-IR signals were well below 2% of the mean equivalent dose for all samples (i.e. 2–7 Gy). As the low residual doses of the pIRIR signal are ruled out as reason for possible age overestimation and the influence of thermally unstable components of the OSL signal was minimized (see Section 3.3) an offset in ages can be seen as indicator of incomplete bleaching of the pIRIR signal and overlaps vice versa may be interpreted as indicator for complete resetting of both signals. Fig. 6 shows a comparison of calculated OSL and pIRIR ages.

Quartz ages of same-site samples agree well within 1 sigma standard error. Seven samples of four different sites show agreement of OSL and pIRIR ages within error (Fig. 6). In contrast,
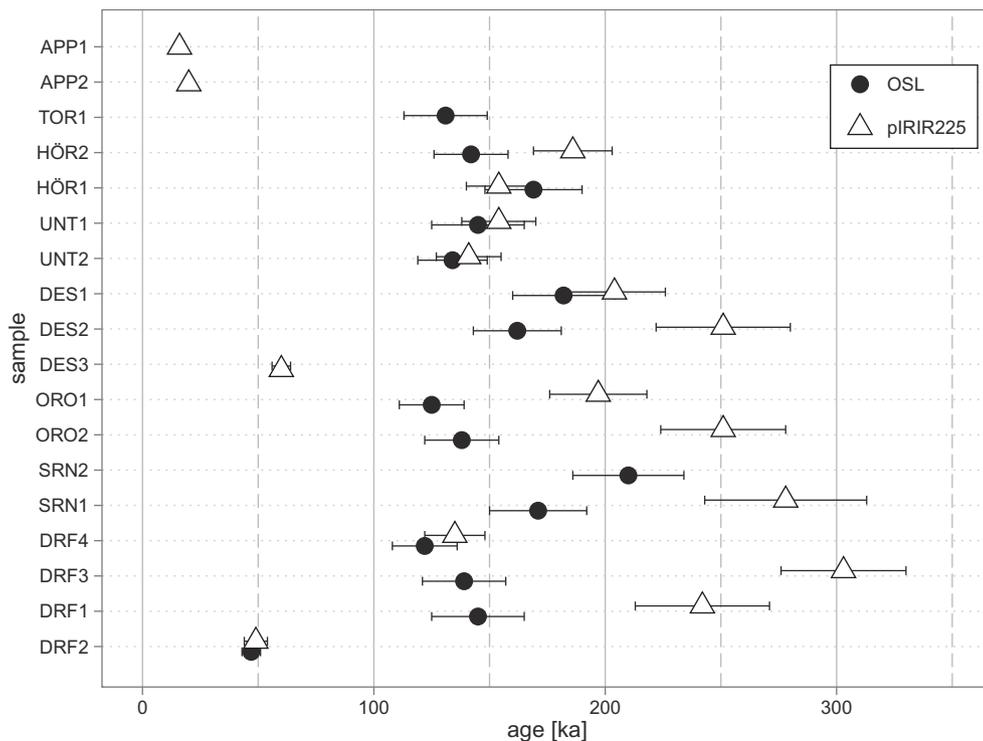

Fig. 6. Comparative plot of calculated central ages (c.f. Galbraith et al., 1999) for Q OSL and KFs pIRIR.

eight samples from five sites show significant offsets between OSL and pIRIR ages. From a methodological viewpoint, offset pIRIR ages are regarded as overestimates due to incomplete bleaching. The bleaching condition of the pIRIR signal of course does not permit conclusions about the resetting state of the quartz signal. In this case, the OSL ages have to be seen in context of stratigraphic and spatial relationships of well bleached samples from the same site or other sites (see Section 4.3).

DRF4 shows agreement between the OSL and the pIRIR age (see Fig. 6), implying complete resetting before burial. Compared to DRF1 and DRF3, for which OSL and pIRIR ages are not consistent within error, the stratigraphic deepest sample DRF4 may act as a reference sample of this site. The quartz OSL ages of DRF1 and DRF3 agree with the pIRIR and OSL age of DRF4. As the outcome of the OSL dating confirms the stratigraphic relationship within the profile, it is reasonable to base further interpretation on the OSL ages. The pIRIR ages of these two samples are overestimating the OSL ages by over 50 ka.

Overdispersion values of OSL and pIRIR D_e distribution are scattered from very low values (<4%) to maximum values of c. 40%. Even though low overdispersions are sometimes seen as indicators for well bleached dose distributions (Olley et al., 2004; Bateman et al., 2008; Neudorf et al., 2012), it has been shown by other authors that this is in fact not mandatory (e.g. Wallinga, 2002). This can be seen especially for very broad, symmetric pIRIR D_e distributions where the pIRIR age overestimates the OSL age by over 100 ka (e.g. DRF3 OSL 139 ± 18, OD 23%; pIRIR 303 ± 27, OD 16%; see also Bickel et al., 2015).

In the following age discussion, interpretations are mainly based on OSL dating results, using the pIRIR ages as qualitative indicators for bleaching completeness. However, for the well bleached samples average quartz OSL and pIRIR ages are in good agreement within error.

4.3. The timing of the penultimate alpine glaciation

4.3.1. Enns-Steyr-Krems valley (sites En1, St1, Kr1)

Nowadays, the Krems valley is separated from the Steyr valley by a watershed. While the ice in the Steyr valley formed an inner alpine valley glacier during the penultimate glaciation, the bulk mass of the ice overflowed the watershed and extended into the alpine foreland of the Krems valley (Kohl and Schmidt, 1985). During the last glacial cycle, the ice did not overflow the watershed and the Krems valley was only under the influence of small localized glaciations (Van Husen, 1975). The absence of a pronounced foreland glaciation in this valley during the last glacial cycle allowed the preservation of several moraine ridges deeply embedded in the pre-penultimate glacial basin. This allows the deduction of several individual glacier extents, whose glaciofluvial meltwater deposits are linked in the foreland deposits of the High Terrace which was sampled at site Kr1. A palyono-logical investigation of a drill core at the Krems/Steyr watershed revealed two parts to the penultimate glaciation in the Krems valley separated by an interstadial with a fern rich picea vegetation (Kohl and Schmidt, 1985). The OSL ages of ORO1 and ORO2 place the accumulation of the Krems High Terrace – and hence the timing of the last phase of the penultimate glaciation, at 138 ± 16 ka (ORO1) and 125 ± 14 ka (ORO2) (Table 2).

From previous investigations (Van Husen, 1975) it is known, that the eastward extending branch of the Krems glacier into the Steyr valley experienced a similar two phased evolution during the penultimate glaciation. In contrast to the Krems valley where terminal moraines define the glacier extents, the extents of the Steyr glacier is assumed from the transition from a very coarse boulder pavement to the glaciofluvial terrace gravels. The samples of site St1 (SRN1, SRN2) yield OSL ages of 171 ± 21 ka and 210 ± 24 ka (Table 2). The main inner-alpine accumulation area for the Steyr and Krems glacier branches were identical; therefore it can be assumed that glacial processes in both valleys were contemporary during the penultimate glaciation, which in turn indicates that the depositional OSL ages of site St1 are overestimating the timing of terrace accumulation – or represents deposits of an earlier glacier advance. In addition, a large offset between OSL and pIRIR – ages as it is the case for SRN2 – may hint towards not only the incomplete resetting of the pIRIR signal but also the OSL signal itself. Therefore we interpret the OSL ages of St1 only as maximum ages for the terrace formation.

A clear connection between terminal moraines at Großraming and the High Terrace deposits in the West is given in the Enns valley (Penck and Brückner, 1909; Van Husen, 1971; Van Husen and Reitner, 2011), confirming that the ice did not extend into the foreland in front of the alpine Enns valley in this period. The largely continuous High Terrace surfaces can be traced from Großraming to the Danube (Van Husen, 1971; Kohl, 2000). Sedimentary evidence proves that before the main ice advance during the penultimate glaciation took place, the east lying Ybbs River drained into the Enns valley (Nagl, 1970; Van Husen, 1971). During the maximum extent of the glacier, this connection was blocked by ice and the Ybbs River changed its path towards north (Untersweg et al., 2012). The terrace deposit of site En1 in the Enns valley is the morphological downstream continuation of the Steyr valley High Terrace of site St1, thus incorporating sediment supply from the alpine Enns and Steyr valley. The OSL ages of the High Terrace at site En1 ($\bar{x}$ DRF1,3,4: 135 ± 12 ka, Table 2) agree well with the ages of High Terrace and ice marginal sediments deposited adjacent to a glacier in decay in the neighbouring Ybbs valley (130 ± 9 ka; Bickel et al., 2015). This implies that the investigated High Terrace deposits of the Krems and Enns valley were formed quasi-synchronous in the same period of time in which the ice decay at the end of the penultimate glaciation in the easternmost Alps happened (c.f. Termination II, Drysdale et al., 2009).

The covering loess DRF2 at the Enns valley site yielded an OSL age of 47 ± 4 ka and a pIRIR age of 49 ± 5 ka (Table 2). Although the quartz age agrees with the KFs age, the dose saturation of quartz was reached for more than 50% of the measured aliquots and was close to 2D0 (c.f. Murray and Wintle, 2003) for the rest of the aliquots. Compared to the glaciofluvial quartz samples, the loess sample DRF2 was exposed to an environmental dose rate nearly three times as high, therefore received a relatively large dose in a shorter time span. Nonetheless, the pIRIR age indicates deposition during the last glacial cycle (Würm), and gives a minimum sedimentation age which generally supports the dating results of the underlying terrace gravels.

4.3.2. Traun valley (sites Tr1, Tr2, Tr3)

Contrary to the large piedmont glaciers in the West (e.g. Salzach, Inn), the Traun glacier branched in several smaller basins (Preusser et al., 2010). Ice transfluence from the Enns glacier and Salzach Glacier existed via intra-montane basins (Mitterndorf Basin, Abtenau Basin; Senarclens-Grancy, 1962). Aside from inner alpine sedimentary provenance, periglacial erosion processes in the north lying Molasse hills (Hausruck, Kobernaußer Wald) had a significant influence on the petrographic composition of the glaciofluvial deposits in the Traun valley (Kohl, 2000). The clearest differentiation between terminal moraines is present at the Traunsee branch. Multiple diachronous moraine ridges were recorded and attributed to three temporally discernible glacier extents from field evidence (Penck and Brückner, 1909; Van Husen, 1977). Each of these terminal moraine systems is connected with a respective High Terrace accumulation, of which only one can be traced from the past glacier front to the Danube. All three investigated sites of the Traun valley (Site Tr1, Tr2, Tr3) are located on this continuous terrace. Quartz OSL dates the two glaciofluvial

Table 2

Dating results of the investigated samples for quartz OSL and K-feldspar pIRIR. Equivalent doses were calculated using the central age models by Galbraith et al. (1999). Ages and errors were calculated using the ADELE software (Kulig, 2005).

Site	Sample	Type	Signal	Mineral	n	D_e [Gy]	OD [%]	Age [ka]
En1	DRF2	Eolian	OSL	Quartz	14	152 ± 10	14	47 ± 4
			pIRIR225	K-feldspar	20	193 ± 11	19	49 ± 5
	DRF1	Glaciofluvial	OSL	Quartz	21	129 ± 12	35	145 ± 20
			pIRIR225	K-feldspar	16	360 ± 28	26	242 ± 29
	DRF3	Glaciofluvial	OSL	Quartz	18	128 ± 9	23	139 ± 18
			pIRIR225	K-feldspar	29	458 ± 20	16	303 ± 27
	DRF4	Glaciofluvial	OSL	Quartz	19	174 ± 8	5	122 ± 14
			pIRIR225	K-feldspar	26	269 ± 7	7	135 ± 13
St1	SRN1	Glaciofluvial	OSL	Quartz	21	109 ± 8	29	171 ± 21
			pIRIR225	K-feldspar	14	337 ± 32	33	278 ± 35
	SRN2	Glaciofluvial	OSL	Quartz	20	145 ± 8	21	210 ± 24
			pIRIR225	K-feldspar	11	486 ± 93	51	420 ± 64
Kr1	ORO2	Glaciofluvial	OSL	Quartz	18	177 ± 9	14	125 ± 14
			pIRIR225	K-feldspar	20	398 ± 22	21	197 ± 21
	ORO1	Glaciofluvial	OSL	Quartz	20	161 ± 8	17	138 ± 16
			pIRIR225	K-feldspar	18	437 ± 26	22	251 ± 27
Tr1	DES3	Eolian	pIRIR225	K-feldspar	20	219 ± 6	5	60 ± 4
	DES2	Glaciofluvial	OSL	Quartz	19	115 ± 8	24	162 ± 19
			pIRIR225	K-feldspar	14	302 ± 26	29	251 ± 29
	DES1	Glaciofluvial	OSL	Quartz	19	126 ± 8	21	182 ± 22
			pIRIR225	K-feldspar	16	258 ± 24	34	204 ± 22
Tr2	UNT2	Glaciofluvial	OSL	Quartz	17	138 ± 12	14	134 ± 15
			pIRIR225	K-feldspar	20	242 ± 12	20	141 ± 14
	UNT1	Glaciofluvial	OSL	Quartz	18	126 ± 11	32	145 ± 20
			pIRIR225	K-feldspar	19	222 ± 13	22	154 ± 16
Tr3	HÖR1	Glaciofluvial	OSL	Quartz	19	130 ± 12	32	169 ± 21
			pIRIR225	K-feldspar	36	197 ± 7	14	154 ± 14
	HÖR2	Glaciofluvial	OSL	Quartz	19	131 ± 13	38	142 ± 16
			pIRIR225	K-feldspar	24	250 ± 9	4	186 ± 17
Sa1	TOR1	Glaciofluvial	OSL	Quartz	17	172 ± 15	27	131 ± 18
			pIRIR225	K-feldspar	–	>600 ±	–	– ± –
Sa2	APP2	Eolian	pIRIR225	K-feldspar	20	50 ±	6	20 ± 2
	APP1	Eolian	pIRIR225	K-feldspar	20	57 ± 2	14	16 ± 2

samples of the most proximal site Tr1 (DES1, DES2) to 187 ± 23 and 169 ± 21 ka. Further downstream at site Tr2, where two samples out of the assumed continuation of the terrace at site Tr1 were collected, OSL ages point towards slightly younger terrace accumulation ages (UNT1 145 ± 20, UNT2 127 ± 15 ka), although DES2 and UNT1 agree within error. Two samples (HOR1, HOR2) of site Tr3, situated on the same morphological terrace body as site Tr2, yield OSL ages of 170 ± 20 and 156 ± 20 ka (Table 2).

The loess sample (DES3) of the proximal site Tr1 yielded a Würmian depositional age (pIRIR) of 60 ± 4 ka. This age is in accordance with the depositional age of the top of a loess sequence 7 km southwest of Tr2 (53 ± 7 ka, uncorrected IRSL; Preusser and Fiebig, 2011). Reworked loess near Tr3 was dated by Terhorst et al. (2002) to a last glacial age between 14.9 and 30.7 ka (Würm) by IRSL-ADD (Additive Dose method).

4.3.3. Salzach valley (sites Sa1, Sa2)

The Salzach glacier was connected to the Inn glacier in the West and the Enns and Traun glaciers in the East and South (Ebers et al., 1966; Kohl, 2000). At least two stages of penultimate glaciation ice extents are recorded by terminal moraine systems in the Salzburg basin (Weinberger, 1955; Ebers et al., 1966). During the most pronounced ice extents, the location of site Sa1 was covered by ice. Interpreted as ice marginal deltaic deposits (Pippan, 1957), these sediments were correlated with the ice decay phase at the end of the penultimate glaciation (Van Husen and Reitner, 2011). The pIRIR age of this site is vastly overestimating the OSL age, exhibiting equivalent doses beyond 600 Gy (∼550 ka). In contrast,

quartz OSL yields an age of 131 ± 18 ka (Table 2), but as the age is from a single sample with no intra-site cross reference, it has to be interpreted with care. Even though the site is only represented by a single age, its chronostratigraphic implications are supported by several other ages from the NAF: the age is in agreement with depositional ages of gravel terraces from the Traun, Krems, and Enns valley in this study and it also agrees with ages of ice marginal deposits and terrace accumulations of the penultimate glaciation in the Ybbs valley (Bickel et al., 2015).

As already mentioned, only the fine grained covering layers of site Sa2 could be sampled, and the age of these provides only a crude minimum age estimate for the terrace accumulation. Due to saturation effects of the OSL signal and high probability of complete signal resetting of the KFs luminescence signal, the pIRIR age was chosen over the Q OSL signal. It revealed an age of 19.9 ± 2.1 ka (APP1) and 16.4 ± 1.7 ka (APP2). This late last glacial age agrees well with uncorrected IRSL ages of the same site (15.7 ± 1.2 ka, Terhorst et al., 2002).

The underlying terrace deposits were dated with uncorrected IRSL by Megies (2006) to 170 ± 20 ka. From experiences gained in the course of this and previous studies (Bickel et al., 2015), it became clear that pIRIR and also low temperature IRSL ages often overestimate the true depositional age of glaciofluvial deposits due to incomplete bleaching. This, and the presence of anomalous fading of the IR50 signal, dictate caution with regard to the reliability of these ages. Terhorst et al. (2002) presented a U/Th age of calcite cements of the same gravel terrace giving a reliable minimum age for the terrace accumulation of 113.4 ± 4.4 ka. From our newly gained data and

aforementioned studies, the presence of a glacier in the Salzach basin area can be temporally constrained between 113.4 ± 4.4 ka and 170 ± 20 ka with deglaciation starting not later than 131 ± 18 ka.

4.4. Regional and supra-regional implications

From luminescence dates gained in this study it is evident that the accumulation of glaciofluvial deposits of the penultimate glaciation in the study area happened between 118 and 175 ka with hints that sediment accumulation culminated around 130–140 ka. Indication exists from dates of sediments typical for ice decay processes (Sa1 site; Ybbs valley, Bickel et al., 2015) that the period of extensive down melting of the glaciers may be time equivalent to late MIS 6/beginning MIS 5 – which implies deposition during Termination II (Drysdale et al., 2009). This means that the main accumulation of the "classic" High Terrace of the Riss (Penck and Brückner, 1909) is time equivalent with MIS 6 as previously proposed by Van Husen (2004) and Van Husen and Reitner (2011). With regards to previous stratigraphic works in this area which proposed repeated glacier advances and retreats during the Riss (e.g. Del-Negro, 1969; Kohl and Schmidt, 1985; Van Husen, 2007), it is not possible to chronologically resolve individual Rissian glacier stands by our luminescence data alone. The ages cover a range of several ten thousand years, so glacier variations on a smaller time scale are unlikely to be resolved. The sites and ages which are discussed in the following are shown in Figs. 7 and 8.

Luminescence and U/Th ages of the glaciofluvial gravel deposits of site Sa2 previously published by Megies (2006) and Terhorst et al. (2002) also strongly suggest an accumulation of the High Terrace during MIS 6. From U/Th investigations of speleothem records from high alpine caves in Austria, it was proposed that ice free conditions in the inner Alps prevailed not later than 125 ka (Spötl and Mangini, 2006). Palynological results of a sediment core drilled in the tongue basin area of the Traun glacier at Lake Mondsee (Van Husen, 2000) placed a sedimentary sequence starting with a Rissian basal till at the bottom overlain by lake sediments in MIS 6 to 3 (Drescher-Schneider, 2000). Palynological and U/Th time constraints for the deglaciation phase and for the following interglacial in the Eastern Alps respectively are also known from Nieselach and Kitzbühel (late MIS 6, Termination II; summarized in Van Husen and Reitner, 2011). Contrary to investigations in the Bavarian NAF where luminescence dating revealed last glacial ages for some High Terrace deposits (Fiebig and Preusser, 2003), all investigated High Terrace gravels in this study are definitely older, belonging to the penultimate glacial cycle.

The dating of the loess samples provided minimum ages for the deposition of the underlying terrace sediments. The order of the sedimentary succession in the field was also represented in the final chronostratigraphic outcome. Nonetheless, a large age gap between the deposition of the gravel terrace and the loess itself is apparent, and prevents any constraint of the glaciofluvial gravel accumulation. As the samples were not collected directly at the loess base and the gravel top, the significance of the age gap is arguable. However, dating results of En1 and Tr1 agree well with IRSL ages of samples collected from loess palaeosol sequences in the Traun valley (Terhorst et al., 2002; Preusser and Fiebig, 2011).

A chronological evolution comparable to that of the NAF was revealed by palynostratigraphic investigations in the south-eastern alpine foreland (Italy) from the Azzano Decimo core by Pini et al. (2009), which contains a sedimentary succession of marine to continental origin. In this study, culmination of the penultimate glaciation was correlated with late MIS 6 with an estimated duration of less than 13 ka. U/Th dates of a stalagmite record in the Apuan Alps propose that interglacial conditions in southern Europe were reached at 129 ± 1 ka (Drysdale et al., 2005) which is in good agreement with speleothem data from the Eastern Alps (Spötl and Mangini, 2006, 2007). The onset of last interglacial conditions in the Mediterranean area (Lago Grande di Monticchio, S-Italy) was dated to 127.2 ka with a quickly progressing transition period (3.35 ka) following the penultimate glaciation (Allen and Huntley, 2009).

The penultimate glaciation of the Central Alps is also documented by large erratic boulders of alpine origin in the Swiss Jura Mountains which revealed surface exposure ages inferred from in situ produced cosmogenic nuclides (10Be) between 126 and 184 ka (Ivy-Ochs et al., 2006; Graf et al., 2007). This chronologically ties the western alpine penultimate glaciation and its subsequent deglaciation phase in the Swiss lowlands to MIS 6. A multi-dating approach on proglacial delta sediments of Landiswil confirmed that the Rhône glacier was present at this site between 153 ± 16 and 160 ± 14 ka (Dehnert et al., 2010). The delta succession was subsequently overrun by an advancing Aare glacier which merged with the Rhône glacier (Gruner, 2001), implying that the ages gained from this site pre-date the maximum extent of the penultimate glaciation. The age of the Swiss penultimate glaciation (Beringen) was also derived from proglacial lake sediments from sediment cores (Niederweningen; Anselmetti et al., 2010; Dehnert et al., 2012), implying the presence of a glacier in the area between 130 and 180 ka. A complex Middle to Late Pleistocene sedimentary successions of the Central Alps is exposed at Thalgut, Switzerland, which comprises sedimentary and palynological evidence for multiple glacials and interglacials (Schlüchter, 1989). The final stage of the penultimate glaciation (coarse delta foresets), subsequent deglaciation and deposition during interglacial conditions (fluviola-custrine deposits) was stored in the sedimentary record and dated by Preusser and Schlüchter (2004) using luminescence dating on fine grain feldspar and quartz (4–11 μm). OSL revealed ages of 149 ± 13 ka and 135 ± 14 ka in the transitional zone, effectively placing the latest-penultimate glacial phase in late MIS 6/starting MIS 5. Recently, a dating approach (Lowick et al., 2015) using various luminescence methods and signals (OSL/IRSL/pIRIR) for glaciofluvial deposits from the Klettgau area (Switzerland), point towards an extensive sedimentation during the Swiss Beringen glaciation (MIS 6, Fig. 7), therefore covering a similar time frame as the deposits presented in this study.

4.5. Palaeoclimatic implications

Is it possible to draw regional climatic conclusions from our new proposed Riss chronology for the eastern NAF in combination with previous studies of this time slice? Compared with the amount of data and studies dealing with glacial/proglacial processes, chronology and climatic variability of the last glacial maximum (LGM) and Termination I during MIS 2, the data base for the penultimate glacial period and older glaciations in the Alps is sparse. On the one hand, this is due to the fragmentary character of the sedimentary remains – owing to pronounced alteration of the landscape by erosional and depositional processes during the following glaciation. On the other hand, luminescence dates in the higher age ranges (>100 ka) often cover an age range within error that cannot give concise information about short temporal variations on the centennial and millennial scale. In this case, only assumptions about the long-term variability such as glacial-interglacial cycles can be made. Therefore, the only detailed climate models and concepts in existence for glacial periods in the Alps were elaborated for the LGM and subsequent Termination I where the database is much more robust (e.g. Florineth and Schlüchter, 2000). It is not clear however, if these atmospheric models may be applied to the penultimate glaciation as well. From the reconstruction of LGM glacier extents in Europe along with
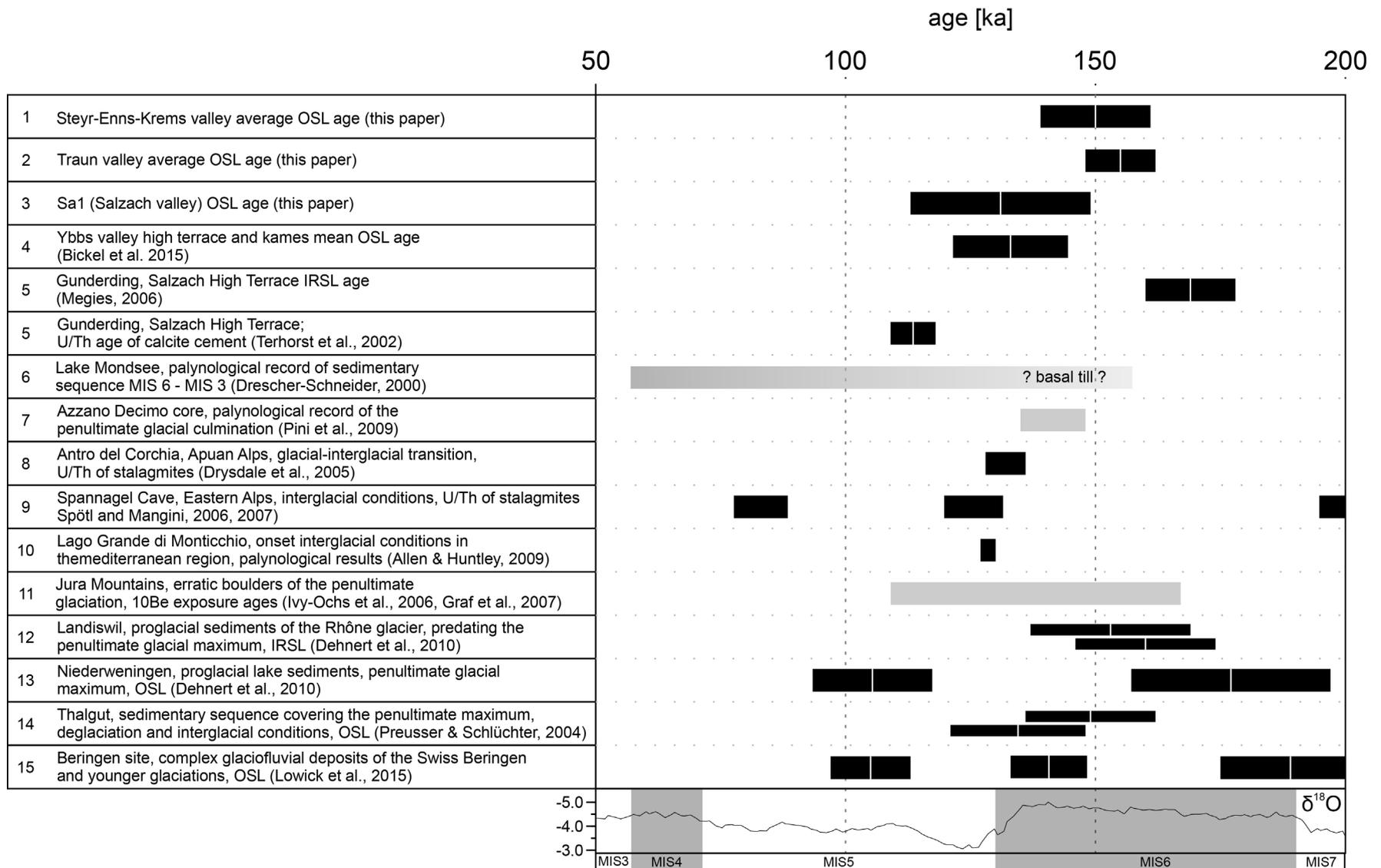
Fig. 7. Comparison of ages gained in this study with ages from sites of the greater circum alpine region. Black blocks indicate the age range the results of the individual studies revealed. Same site sample ages overlapping in error were averaged and the respective standard error is shown by the extent of the black bar while the white line indicates the mean age. The benthic δ18O stack and marine isotope stages (Lisiecki and Raymo, 2005) are provided for better orientation.
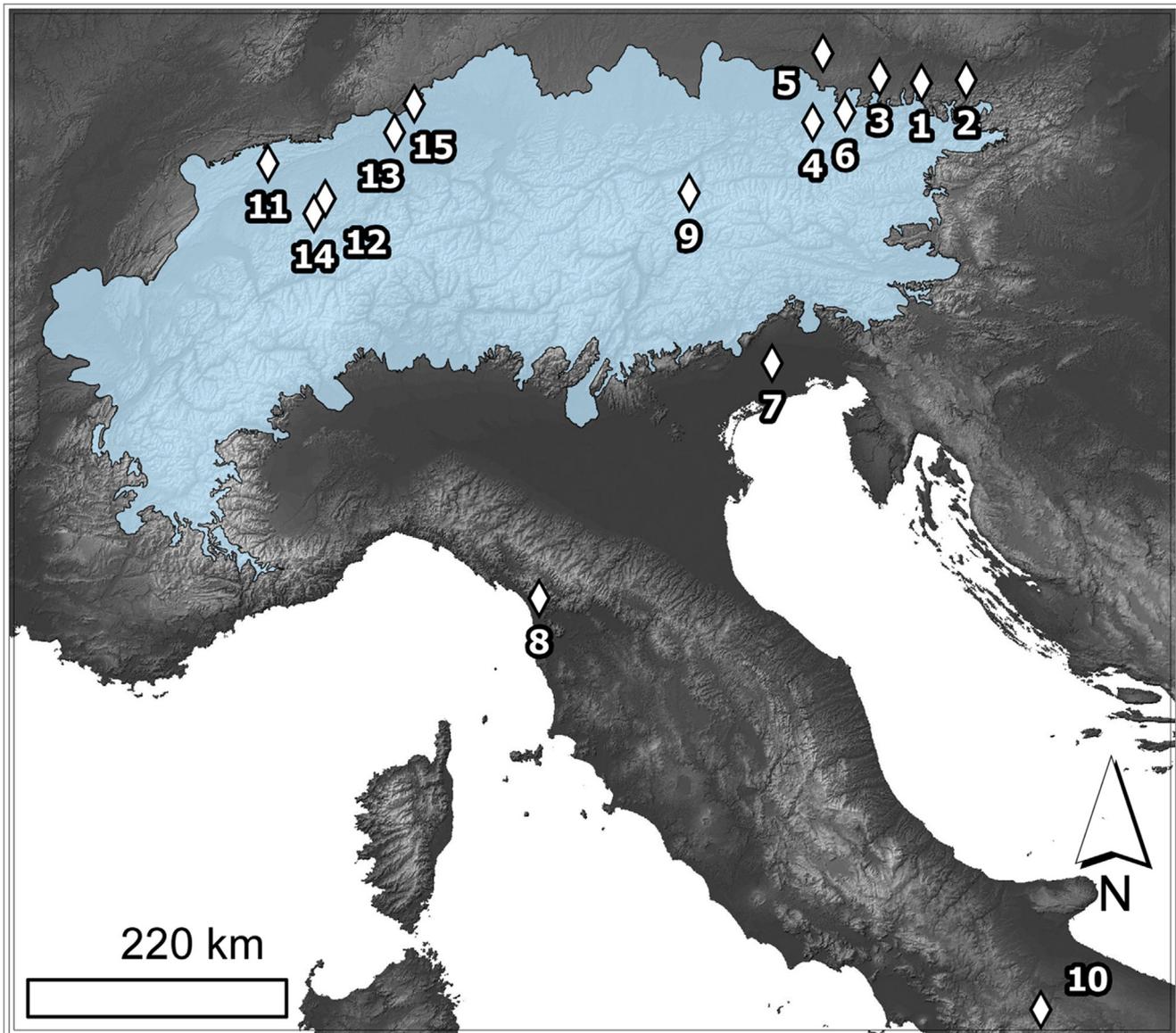
Fig. 8. Map showing the location of the discussed sites. Numbers refer to sites in Fig. 7.

investigations on palaeoclimate records, Florineth and Schlüchter (2000) proposed that the Alps were strongly affected by precipitation delivered by a dominant southern atmospheric circulation. Steep moisture gradients across the Eastern Alps and the Western Carpathians were concluded from comparative palaeobotanical records covering the LGM and MIS 3 (Pini et al., 2010) which resulted in an asymmetric accumulation of ice masses in the Alps. While a comprehensive and detailed data set that would allow an assumption of the same principle for the accumulation phases of the penultimate alpine glacial cycle does not yet exist, although similarities in the course of the deglaciation are evident from geochronological data. The early late-glacial ice decay happened abruptly and almost synchronous in the Alps during Termination I (Reitner, 2007; Ivy-Ochs et al., 2008). Within methodological uncertainties geochronological data generally show that during Termination II ice decay happened rapidly and synchronous (see Section 4.4) – probably similar to Termination I (Reitner, 2007; Ivy-Ochs et al., 2008). For the time slice in question, the data is still fragmentary and so similarities between the last and the penultimate glacial cycle remain debatable. Therefore, it is desirable to consolidate the amount of investigated terrestrial

records of the circumalpine regions. Whereas luminescence ages of proglacial terrace accumulations can give information about the timing of glaciations in the hinterland areas, surface exposure dating on erratic boulders in the foreland might help to elaborate on the potential spatial variability of deglaciation processes after the penultimate glaciation and also give estimates about the maximum glacier extent in the absence of clearly discernible terminal moraines. In this context it is also essential to extend the network of investigated high alpine speleothem records as they are able to deliver precisely dateable, high resolution climate proxies not only for the penultimate but also for older interglacials (Bard et al., 2002; Spötl et al., 2006; Couchoud et al., 2009; Drysdale et al., 2009). In addition, climatic reconstructions from vegetation records based on palyonostratigraphic investigations are an important asset in the process of reconstructing the penultimate glacial climate and its following interglacial period. Hence, an overall alpine record for the penultimate glaciation/interglacial containing high-resolution data spanning the whole alpine area supported by luminescence dated terrestrial archives is the ultimate goal to understand chronological and spatial climatic variability.

5. Conclusions

- 18 samples of glaciofluvial, fluviolacustrine and eolian origin were collected in the Austrian NAF and dated with a twofold luminescence dating approach (Q OSL, KFs pIRIR225). The glaciofluvial and fluviolacustrine sediments were previously assumed to correlate with the Riss glaciation (penultimate glaciation).

- Quartz generally displays better resetting of the signal compared to feldspar but complete resetting of the luminescence signal can only be assured when central ages for both signals agree.

- The OSL ages in this study which were used for chronostratigraphic interpretations show that the deposition of the glaciofluvial sediments was most likely time equivalent with MIS 6 with indication that the culmination of the penultimate glaciation happened in late MIS 6.

- A twofold Rissian glaciation characterized by significantly differing ice extents as previously suggested was not apparent from the reported ages. Still, this does not negate the possibility that short-term cyclical changes occurred (Van Husen and Reitner, 2011) which are below the technical resolution limit of the luminescence dating approach.

- The transition from glacial to deglaciation and interglacial conditions was most likely relatively fast as indicated by data in this study and from other sedimentary archives (Drysdale et al., 2005; Spötl and Mangini, 2006; Spötl et al., 2006; Pini et al., 2009) and happened in late MIS 6/starting MIS 5.

- Luminescence ages and their respective uncertainty in this age range allow to distinguish interglacial-glacial cycles, but unfortunately is unable to resolve this particular period to a higher degree (e.g. stadial-interstadial).

- It is not known why the minerals from the Austrian NAF investigated in this study provide consistent dating results while minerals from other parts of the NAF do not (e.g. Klasen, 2008). Further studies should investigate this open question, also considering using a multi mineral-multi signal approach.

Acknowledgements

Appendix A. Supplementary data

Supplementary data associated with this article can be found, in the online version, at http://dx.doi.org/10.1016/j.pgeola.2015.08.002. These data include Google maps of the most important areas described in this article.

References

Agassiz, L., 1841. Untersuchungen über die Gletscher (Investigations of the glaciers). , pp. 338.

Aitken, M.J., 1998. An Introduction to Optical Dating: The Dating of Quaternary Sediments by the Use of Photon-stimulated Luminescence. Oxford University Press, Oxford and New York.

Allen, J.R.M., Huntley, B., 2009. Last Interglacial palaeovegetation, palaeoenvironments and chronology: a new record from Lago Grande di Monticchio, southern Italy. Quaternary Science Reviews 28, 1521–1538, http://dx.doi.org/10.1016/j.quascirev.2009.02.013.

Anselmetti, F.S., Drescher-Schneider, R., Furrer, H., Graf, H.R., Lowick, S.E., Preusser, F., Riedi, M.A., 2010. A ~180 000 years sedimentation history of a perialpine overdeepened glacial trough (Wehntal, N-Switzerland). Swiss Journal of Geosciences 103, 345–361, http://dx.doi.org/10.1007/s00015-010-0041-1.

Auclair, M., Lamothe, M., Huot, S., 2003. Measurement of anomalous fading for feldspar IRSL using SAR. Radiation Measurements 37, 487–492.

Bailey, R.M., Arnold, L., 2006. Statistical modelling of single grain quartz De distributions and an assessment of procedures for estimating burial dose. Quaternary Science Reviews 25, 2475–2502.

Bard, E., Antonioli, F., Silenzi, S., 2002. Sea-level During the Penultimate Interglacial Period Based on a Submerged Stalagmite from Argentarola Cave (Italy) p. 196.

Bateman, M.D., Carr, A.S., Murray-Wallace, C.V., Roberts, D.L., Holmes, P.J., 2008. A dating intercomparison study on Late Stone Age coastal midden deposits, South Africa. Geoarchaeology 23, 715–741, http://dx.doi.org/10.1002/gea.20243.

Bickel, L., Lüthgens, C., Lomax, J., Fiebig, M., 2015. Luminescence dating of glaciofluvial deposits linked to the penultimate glaciation in the Eastern Alps. Quaternary International 357, 110–124, http://dx.doi.org/10.1016/j.quaint.2014.10.013.

Bøtter-Jensen, L., McKeever, S.W.S., Wintle, A.G., 2003. Optically Stimulated Luminescence Dosimetry. Elsevier, Amsterdam.

Bridge, J.S., Lunt, I.A., 2006. Depositional models of braided riversIn: Braided Rivers: Process, Deposits, Ecology and Management, pp. 11–50, http://dx.doi.org/10.1002/9781444304374 (Chapter 2).

Buylaert, J.P., Murray, A.S., Thomsen, K.J., Jain, M., 2009. Testing the potential of an elevated temperature IRSL signal from K-feldspar. Radiation Measurements 44, 560–565.

Couchoud, I., Genty, D., Hoffmann, D., Drysdale, R., Blamart, D., 2009. Millennial-scale climate variability during the Last Interglacial recorded in a speleothem from south-western France. Quaternary Science Reviews 28, 3263–3274, http://dx.doi.org/10.1016/j.quascirev.2009.08.014.

Dehnert, A., Lowick, S., Preusser, F., Anselmetti, F., Drescher-Schneider, R., Graf, H., Heller, F., Horstmeyer, H., Kemna, H., Nowaczyk, N., Züger, A., Furrer, H., 2012. Evolution of an overdeepened trough in the northern Alpine Foreland at Niederweningen, Switzerland. Quaternary Science Reviews 34, 127–145.

Dehnert, A., Preusser, F., Kramers, J.D., Akçar, N., Kubik, P.W., Reber, R., Schlüchter, C., 2010. A multi-dating approach applied to proglacial sediments attributed to the Most Extensive Glaciation of the Swiss Alps. Boreas 39, 620–632.

Del-Negro, W., 1969. Bemerkungen zu den Kartierungen L Weinbergers im Traungletschergebiet (Atter- und Traunseebereich). Abhandlungen der Geologischen Bundesanstalt 1, 12–15.

Drescher-Schneider, R., 2000. Die Vegetations- und Klimaentwicklung im Riß/Würm-Interglazial und im Früh- und Mittelwürm in der Umgebung von Mondsee, Ergebnisse der pollenanalytischen Untersuchungen. In: Van Husen, D. (Ed.), Klimaentwicklung Im Riss/Würm Interglazial (Eem) Und Frühwürm (Sauerstoffisotopenstufe 6-3) in Den Ostalpen. Verlag der Österreichischen Akademie der Wissenschaften, pp. 39–92.

Drysdale, R.N., Hellstrom, J.C., Zanchetta, G., Fallick, A.E., Sánchez Goñi, M.F., Couchoud, I., McDonald, J., Maas, R., Lohmann, G., Isola, I., 2009. Evidence for obliquity forcing of glacial Termination II. Science 325, 1527–1531, http://dx.doi.org/10.1126/science.1170371.

Drysdale, R.N., Zanchetta, G., Hellstrom, J.C., Fallick, A.E., Zhao, J., 2005. Stalagmite evidence for the onset of the Last Interglacial in southern Europe at 129 ± 1 ka. Geophysical Research Letters 32, L24708, http://dx.doi.org/10.1029/2005GL024658.

Ebers, E., Weinberger, L., Del-Negro, W., 1966. Der Pleistozäne Salzachvorlandgletscher, Veröffentl. ed. Gesellschaft für Bayerische Landeskunde e.V., München.

Ehlers, J., Gibbard, P.L. (Eds.), 2004. Quaternary Glaciations-extent and Chronology: Part I: Europe. Elsevier.

Ellwanger, D., Wielandt-Schuster, U., Franz, M., Simon, T., 2011. The Quaternary of the southwest German Alpine Foreland (Bodensee-Oberschwaben, Baden-Württemberg, Southwest Germany). Eiszeitalter und Gegenwart Quaternary Science Journal 60, 306–328.

Fiebig, M., Preusser, F., 2003. Das Alter fluvialer Ablagerungen aus der Region Ingolstadt (Bayern) und ihre Bedeutung für die Eiszeitenchronologie des Alpenvorlandes. Zeitschrift für Geomorphologie N.F. 47, 449–467.

Florineth, D., Schlüchter, C., 2000. Alpine evidence for atmospheric circulation patterns in Europe during the Last Glacial Maximum. Quaternary Research 54, 295–308, http://dx.doi.org/10.1006/qres.2000.2169.

Galbraith, R., Roberts, R., Laslett, G., Yoshida, H., Olley, J., 1999. Optical dating of single and multiple grains of quartz from Jinmium Rock Shelter, Northern Australia: Part I. Experimental design and statistical models. Archaeometry 41, 339–364.

Graf, A.A., Strasky, S., Ivy-Ochs, S., Akçar, N., Kubik, P.W., Burkhard, M., Schlüchter, C., 2007. First results of cosmogenic dated pre-Last Glaciation erratics from the Montoz area, Jura Mountains, Switzerland. Quaternary International 164–165, 43–52, http://dx.doi.org/10.1016/j.quaint.2006.12.022.

Gruner, U., 2001. Erläuterungen zu Blatt 1167 Worb-Geologischer Atlas der Schweiz 1:25 000.

Huntley, D., Baril, M., 1997. The K content of the K-feldspars being measured in optical and thermoluminescence dating. Ancient TL 15, 11–13.

Huntley, D., Lamothe, M., 2001. Ubiquity of anomalous fading in K-feldspars and the measurement and correction for it in optical dating. Canadian Journal of Earth Science 38, 1093–1106.

Ivy-Ochs, S., Kerschner, H., Reuther, A., Maisch, M., Sailer, R., Schaefer, J., Kubik, P.W., Synal, H., Schlüchter, C., 2006. The timing of glacier advances in the northern European Alps based on surface exposure dating with cosmogenic 10Be, 26Al, 36Cl, and 21Ne. Geological Society of America: Special Paper 415, 43–60.

Ivy-Ochs, S., Kerschner, H., Reuther, A., Preusser, F., Heine, K., Maisch, M.A.X., Kubik, P.W., Schlüchter, C., 2008. Chronology of the last glacial cycle in the European Alps. Journal of Quaternary Science 23, 559–573, http://dx.doi.org/10.1002/jqs.

Kars, R.H., Reimann, T., Ankjaergaard, C., Wallinga, J., 2014. Bleaching of the post-IR IRSL signal: new insights for feldspar luminescence dating. Boreas, http://dx.doi.org/10.1111/bor.12082.

King, G.E., Robinson, R.A., Finch, J.A.A., 2014. Towards successful OSL sampling strategies in glacial environments: deciphering the influence of depositional processes on bleaching of modern glacial sediments from Jostedalen, Southern Norway. Quaternary Science Reviews 89, 94–107, http://dx.doi.org/10.1016/j.quascirev.2014.02.001.

Klasen, N., 2008. Lumineszenzdatierung glazifluvialer Sedimente im nördlichen Alpenvorland (Luminescence dating of glaciofluvial sediments in the Northern Alpine Foreland). PhD Thesis, University of Cologne 177p.

Kohl, H., 2000. Das Eiszeitalter in Oberösterreich, Schriftenr. ed. Oberösterreichischer Museumverein, Linz. 487p.

Kohl, H., Schmidt, K., 1985. Ein quartärgeologisch interessantes Bohrprofil im Wasserscheidenbereich zwischen den Flüssen Krems und Steyr (Oberösterreich). Jahrbuch des Oberösterreichischen Musealvereines 130a, 149–160.

Krenmayr, H., Schnabel, W., Reitner, J.M., 2006. Geological map of Upper Austria, 1:200.000 1 sheet, 2 additional maps.

Kulig, G., 2005. Erstellung einer Auswertesoftware zur Altersbestimmung mittels Lumineszenzverfahren. TU Freiberg.

Lisiecki, L., Raymo, M., 2005. A Pliocene-Pleistocene stack of 57 globally distributed benthic δ 18 O records. Paleoceanography 20.

Lowick, S.E., Buechi, M.W., Gaar, D., Graf, H.R., Preusser, F., 2015. Luminescence dating of Middle Pleistocene proglacial deposits from northern Switzerland: methodological aspects and stratigraphical conclusions. Boreas 44, 459–482, http://dx.doi.org/10.1111/bor.12114.

Lüthgens, C., Böse, M., Lauer, T., Krbetschek, M., Strahl, J., Wenske, D., 2011. Timing of the last interglacial in Northern Europe derived from Optically Stimulated Luminescence (OSL) dating of a terrestrial Saalian–Eemian–Weichselian sedimentary sequence in NE-Germany. Quaternary International 241, 79–96, http://dx.doi.org/10.1016/j.quaint.2010.06.026.

Lüthgens, C., Krbetschek, M., Böse, M., Fuchs, M.C., 2010. Optically stimulated luminescence dating of fluvioglacial (sandur) sediments from north-eastern Germany. Quaternary Geochronology 5, 237–243, http://dx.doi.org/10.1016/j.quageo.2009.06.007.

Megies, H., 2006. Kartierung, Datierung und umweltgeschichtliche Bedeutung der jungquartären Flussterrassen am unteren Inn (Mapping, Dating and Ecohistorical Importance of Lower Quaternary Fluvial Terraces of the Lower Inn). Heidelberger Geographische Arbeiten 207p.

Miall, A.D., 2006. The Geology of Fluvial Deposits – Sedimentary Facies, Basin Analysis, and Petroleum Geology, 4th ed. Springer 582p.

Miara, S., 1996. Deckschichtenuntersuchungen zur Gliederung der Rißeiszeit beiderseits der Iller im Gebiet des Rhein- und Illergletschers (westliches Alpenvorland/Deutschland). Jahresberichte und Mitteilungen des Oberrheinischen Geologischen Vereins 78, 359–374, http://dx.doi.org/10.1127/jmogv/78/1996/359.

Murray, A.S., Wintle, A.G., 2003. The single aliquot regenerative dose protocol: potential for improvements in reliability. Radiation Measurements 37, 377–381.

Murray, a., Thomsen, S., Masuda, K.J., Buylaert, N., Jain, J.P.M., 2012. Identifying well-bleached quartz using the different bleaching rates of quartz and feldspar luminescence signals. Radiation Measurements 47, 688–695, http://dx.doi.org/10.1016/j.radmeas.2012.05.006.

Nagl, H., 1970. Zur Rekonstruktion der pleistozänen Vereisung im alpinen Ybbstal.(-About the reconstruction of the Pleistocene glaciation of the alpine Ybbs valley). Mitteilungen der Geologischen Gesellschaft Wien 63, 185–202.

Neudorf, C.M., Roberts, R.G., Jacobs, Z., 2012. Sources of overdispersion in a K-rich feldspar sample from north-central India: insights from De K content and IRSL age distributions for individual grains. Radiation Measurements 47, 696–702, http://dx.doi.org/10.1016/j.radmeas.2012.04.005.

Olley, J.M., Pietsch, T., Roberts, R.G., 2004. Optical dating of Holocene sediments from a variety of geomorphic settings using single grains of quartz. Geomorphology 60, 337–358, http://dx.doi.org/10.1016/j.geomorph.2003.09.020.

Penck, A., Brückner, E., 1909. Die Alpen im Eiszeitalter/Bd. 1. Die Eiszeiten in den nördlichen Ostalpen(The Alps during the ice age/Vol. 1. The ice age in the northern Eastern Alps). p. 393.

Pini, R., Ravazzi, C., Donegana, M., 2009. Pollen stratigraphy, vegetation and climate history of the last 215 ka in the Azzano Decimo core (plain of Friuli, north-eastern Italy). Quaternary Science Reviews 28, 1268–1290, http://dx.doi.org/10.1016/j.quascirev.2008.12.017.

Pini, R., Ravazzi, C., Reimer, P.J., 2010. The vegetation and climate history of the last glacial cycle in a new pollen record from Lake Fimon (southern Alpine foreland, N-Italy). Quaternary Science Reviews 29, 3115–3137, http://dx.doi.org/10.1016/j.quascirev.2010.06.040.

Pippan, T., 1957. Bericht 1956 über geologische Aufnahmen auf den Blättern Hallein (94/1) und Untersberg (93/2), 1:25.000. Verhandlungen der Geologischen Bundesanstalt 52–56.

Prescott, J., Hutton, J., 1994. Cosmic ray contributions to dose rates for luminescence and ESR dating: large depths and long-term time variations. Radiation Measurements 23, 497–500.

Preusser, F., Schlüchter, C., 2004. Dates from an important early Late Pleistocene ice advance in the Aare valley, Switzerland. Eclogae Geologicae Helvetiae 97, 245–253, http://dx.doi.org/10.1007/s00015-004-1119-4.

Preusser, F., Degering, D., Fuchs, M., Hilgers, A., Kadereit, A., Klasen, N., Krbetschek, M., Richter, D., Spencer, J., 2008. Luminescence dating: basics, methods and applications. Eiszeitalter und Gegenwart Quaternary Science Journal 57, 95–149.

Preusser, F., Reitner, J.M., Schlüchter, C., 2010. Distribution, geometry, age and origin of overdeepened valleys and basins in the Alps and their foreland. Swiss Journal of Geosciences 103, 407–426, http://dx.doi.org/10.1007/s00015-010-0044-y.

Preusser, F., Fiebig, M., 2011. Chronologische Einordnung des Lössprofi ls Wels auf der Basis von Lumineszenzdatierungen. Mitteilungen der Kommission für Quartärforschung der Österreichischen Akademie der Wissenschaften 63–70.

Reitner, J.M., 2007. Glacial dynamics at the beginning of Termination I in the Eastern Alps and their stratigraphic implications. Quaternary International 164–165, 64–84, http://dx.doi.org/10.1016/j.quaint.2006.12.016.

Rhodes, E., 2011. Optically stimulated luminescence dating of sediments over the past 200,000 years. Annual Review of Earth and Planetary Sciences 39, 461–488.

Roskosch, J., Winsemann, J., Polom, U., Brandes, C., Tsukamoto, S., Weitkamp, A., Bartholomäus, W., Henningsen, A.D., Frechen, M., 2015. Luminescence dating of ice-marginal deposits in northern Germany: evidence for repeated glaciations during the Middle Pleistocene (MIS 12 to MIS 6). Boreas 44, 103–126, http://dx.doi.org/10.1111/bor.12083.

Schlüchter, C., 1989. Thalgut: Ein umfassendes eiszeitstratigraphisches Referenzprofil im nördlichen Alpenvorland. Eclogae Geologicae Helvetiae 277–284.

Schuster, R., Daurer, A., Krenmayr, H.G., Linner, M., Mandl, G.W., Pestal, G., Reitner, J.M., 2014. Rocky Austria. Geologische Bundesanstalt (GBA) 80p.

Senarclens-Grancy, W., 1962. Beiträge zur Eingliederung der Moränen der Schladminger Tauern, der Mitterennstaler Moore un der Ramsau- oder Ennstalterrasse bei Schladming in das alpine Jungquartär. Jahrbuch der Geologischen Bundesanstalt 105.

Spötl, C., Holzkämper, S., Mangini, A., 2006. The last and the penultimate interglacial as recorded by speleothems from a climatically sensitive high-elevation cave site in the Alps. Developments in Quaternary Science 7, 471–491.

Spötl, C., Mangini, A., 2006. U/Th age constraints on the absence of ice in the central Inn Valley (eastern Alps, Austria) during Marine Isotope Stages 5c to 5a. Quaternary Research 66, 167–175.

Spötl, C., Mangini, A., 2007. Speleothems and paleoglaciers. Earth and Planetary Science Letters 254, 323–331.

Starnberger, R., Rodnight, H., Spötl, C., 2013. Luminescence dating of fine-grain lacustrine sediments from the Late Pleistocene Unterangerberg site (Tyrol, Austria). Austrian Journal of Earth Science 106, 4–15.

Terhorst, B., Frechen, M., Reitner, J.M., 2002. Chronostratigraphische Ergebnisse aus Lößprofilen der Inn- und Traun-Hochterrassen in Oberösterreich. Zeitschrift für Geomorphologie Supplement Issues 127, 213–232.

Thrasher, I.M., Mauz, B., Chiverrell, R.C., Lang, A., 2009. Luminescence dating of glaciofluvial deposits: a review. Earth: Science Review 97, 133–146.

Untersweg, T., Wimmer-Frey, I., Heinrich, M., Pfleiderer, S., Reitner, H., 2012. Pleistocene ice extent in the upper Ybbs valley in Lower Austria. Quaternary International 279–280, 508.

Van Husen, D., 1971. Zum Quartär des unteren Ennstales Von Großraming bis zur Donau. Verhandlungen der Geologischen Bundesanstalt 1971, 511–521.

Van Husen, D., 1975. Die Quartäre Entwicklung des Steyrtales und seiner Nebentäler. Jahrbuch des Oberösterreichischen Musealvereines 120, 271–289.

Van Husen, D., 1977. Zur Fazies und Stratigraphie der jungpleistozänen Ablagerungen im Trauntal, pp. 1–130.

Van Husen, D., 2000. Die Paläogeographische Situation des Mondsees im Riss/Würm Interglazial und Frühwürm. In: van Husen, D. (Ed.), Klimaentwicklung Im Riss/Würm Interglazial (Eem) Und Frühwürm (Sauerstoffisotopenstufe 6-3) in Den Ostalpen. Verlag der Österreichischen Akademie der Wissenschaften, pp. 9–12.

Van Husen, D., 2004. Quaternary glaciations in Austria. Developments in Quaternary Science 2, 1–13.

Van Husen, D., 2007. Landschaftsgestaltung durch die Eiszeiten. In: Egger, H. (Ed.), Geologische Karte Der Republik Österreich 1:50 000 Erläuterungen Zu Blatt 67 Grünau Im Almtal. Geologische Bundesanstalt (GBA), Vienna, pp. 12–14.

Van Husen, D., 2011a. Landschaftsgestaltung durch die Eiszeiten. In: Egger, H., van Husen, D. (Eds.), Geologische Karte Der Republik Österreich 1:50,000; Erläuterungen Zu Blatt 69 Grossraming. Geologische Bundesanstalt (GBA), pp. 11–17.

Van Husen, D., 2011b. Quartär bis oberstes Neogen. In: Rupp, C., Linner, M., Mandl, G.W. (Eds.), Geologische Karte von Oberösterreich 1:200.000 – Erläuterungen. Geologische Bundesanstalt (GBA), Vienna, Austria, 255p.

Van Husen, D., Reitner, J., 2011. An outline of the quaternary stratigraphy of Austria. Eiszeitalter und Gegenwart Quaternary Science Journal 60, 366–387.

Wallinga, J., 2002. On the detection of OSL age overestimation using single-aliquot techniques. Geochronometria 21, 17–26.

Weinberger, L., 1955. Exkursion durch das österreichische Salzachgletschergebiet und die Moränengürtel der Irrsee-und Attersee-Zweige des Traungletschers. Verhandlungen der Geologischen Bundesanstalt Sonderheft 7–34.

Wintle, A.G., 1977. Detailed study of a thermoluminescent mineral exhibiting anomalous fading. Journal of Luminescence 15, 385–393.

Wintle, A.G., Murray, A.S., 2006. A review of quartz optically stimulated luminescence characteristics and their relevance in single-aliquot regeneration dating protocols. Radiation Measurements 41, 369–391.